Chapter 3

Formation Mechanism and Elimination of Small-Angle Grain Boundary in AlN Grown on (0001) Sapphire Substrate

Ryan G. Banal, Masataka Imura and Yasuo Koide

Additional information is available at the end of the chapter

http://dx.doi.org/10.5772/66177

Abstract

AlN epilayers were grown on (0001) sapphire substrates by metal-organic vapor phase epitaxy (MOVPE), and the influence of substrate's surface structure on the formation of in-plane rotation domain is studied. The surface structure of sapphire substrate is found to change during thermal cleaning and temperature ramp-up. The oxygen-terminated surface with monolayer (ML) steps having *ABAB* stacking is attributed to cause the formation of a small-angle grain boundary (SAGB). To suppress the formation of such a special grain boundary, the two-step temperature growth technique was employed. It was found that a proper timing of the low-temperature buffer layer (LT BL) growth is necessary to eliminate the SAGB. Moreover, the BL growth temperature (T_g) is also found to affect the surface morphology and structural quality of AlN epilayer. The optimized LT BL T_g is found to be 1050°C. The optical emission property by cathodoluminescence (CL) measurements showed higher emission intensity from AlN epilayer without SAGB.

Keywords: small-angle grain boundary, SAGB, AlN, sapphire substrate, MOVPE, cathodoluminescence, deep-UV, two-step temperature growth

1. Introduction

Single crystal sapphire with corundum structure is a widely used substrate for film deposition and epitaxial growth in many technological fields, such as in optoelectronics for the growth of AlN, GaN, and InN nitride materials. This material exhibits high melting point (2050°C), extremely high chemical stability even at high temperatures, and transparency in the

ultraviolet (UV) region, making it a suitable substrate especially for the growth of AlN, which requires high temperature above 1200°C due to the high viscosity of Al atoms. Sapphire also exhibits a hardness of 9 in the Mohs scale, compared to 10 for diamond. On the other hand, AlN is a promising material for UV and deep-UV light emitters and power electronic devices because of its wide bandgap energy (6.05 eV), good stability at elevated temperature, high thermal conductivity (3.4 $W \cdot cm^{-1} \cdot K^{-1}$) and high electric breakdown field (11.7×10^6 $V \cdot cm^{-1}$). Although the native bulk AlN or GaN substrates are already available for homoepitaxial growths, the utilization of sapphire as the substrate material for heteroepitaxial growth of AlN, GaN, InN, and other emerging materials is expected for the years to come, owing to its mature growth technology, availability of large size wafer, and cost advantage [1–2]. In fact, the advances in heteroepitaxial growths have already successfully demonstrated deep-UV light-emitting diodes (LEDs) and photo-pumped AlGaN multi-quantum well lasers [3–7]. However, the radiative emission efficiencies of deep-UV light emitters are still low, prompting for further reduction of dislocations that act as nonradiative recombination centers [3–6].

The heteroepitaxial growth of AlN on sapphire substrate induces several types of dislocations that are driven by their lattice mismatch and difference in crystal structure. With lattice mismatch, a pseudomorphic growth initially occurs, followed by misfit dislocations after exceeding the critical thickness for plastic relaxation. A 30° rotation of AlN epilayer with respect to sapphire substrate in the basal (0001) plane occurs [8]. However, the development of various growth methods has improved the epitaxial quality of AlN in recent years. These growth methods include alternating supply of source precursors (e.g., modified migration-enhanced epitaxy (MEE)) [9–15], direct and high-temperature growth [16–18], substrate pretreatment (e.g., nitridation) [19, 20], two-step low-temperature (LT) AlN buffer layer (BL) and high-temperature (HT) growth [15, 21–23], multiple-step V/III growth [18, 24], precursor preflow [25], and so on. However, despite the improvement in the surface morphology and structural quality of AlN epilayer, the existence of in-plane rotation domain as exhibited by small-angle grain boundary (SAGB) is still observed, regardless of growth method employed [16, 19–21, 25, 26]. This kind of defect must be eliminated as it can have a negative impact in the optical as well as electrical properties of the devices by acting as barriers for transport or carrier sinks. Small-angle grain boundary is one type of special grain boundary which results when the two crystals have only a slight misorientation relative to each another. Moreover, this kind of special grain can be characterized as pure low-angle tilt boundary or pure low-angle twist boundary, where the former is composed of an array of parallel edge dislocations, while the latter is characterized as the slight rotation of crystals about a common axis which is normal to the plane of the boundary.

2. Origin of small-angle grain boundary (SAGB)

The SAGB in AlN grown on (0001) sapphire substrate is considered to originate from the substrate's surface structure. As in any heteroepitaxial growth, the surface structure influences the growth mode. For example, the appearance of a defect structure on the substrate surface (e.g., protrusion) could possibly lead to spiral growth. It is therefore

http://dx.doi.org/10.5772/66177

necessary to keep the surface free from any defects as possible. However, as-received sapphire substrates are not free from any surface defects even after undergoing polishing treatment. This includes scratches on the surface, as shown in **Figure 1(a)**. Hence, thermal cleaning under H_2 ambient is performed prior to AlN growth either at the same AlN growth temperature or slightly above it. After thermal cleaning, the substrate's surface transformed into parallel step-and-terrace structure as shown in **Figure 1(b)**. The estimated step height from the line scan is about 0.21 nm.

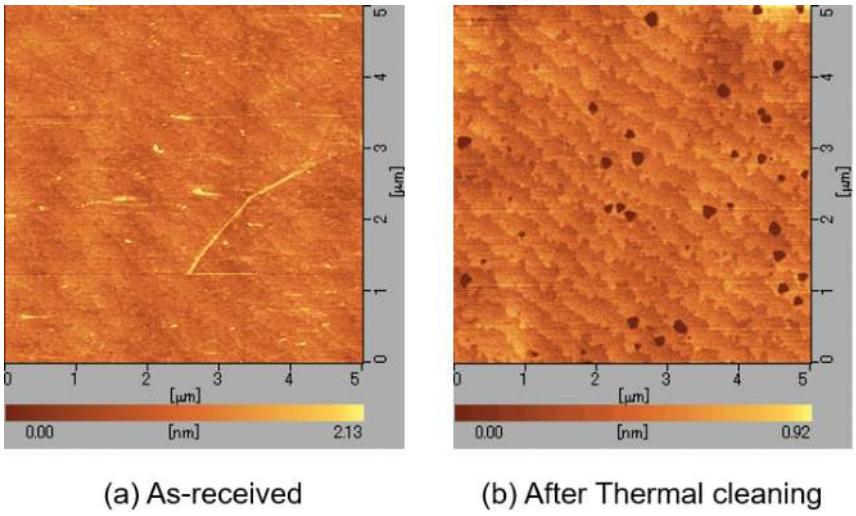

Figure 1. AFM surface morphology of (a) as-received and (b) after thermally cleaned sapphire substrate under H_2 ambient (Ph.D. Thesis, R.G. Banal, Kyoto University).

The crystal lattice of sapphire (α-Al_2O_3) is formed by Al^{3+} and O^{2-} ions. In Al_2O_3 corundum structure, O^{2-} ions are shifted slightly from the idealized hexagonal close-packed positions within the (0001) basal plane due to the empty octahedral sites (note that only two out of every three octahedral sites are occupied by Al^{3+} cations) as shown in **Figure 2(a)** [27, 28]. This results in the formation of two distorted oxygen hexagonal layers as also indicated in **Figure 2(a)** appearing alternately along the [0001] direction with monolayer (ML) periodicity (**Figure 2(b)**). The two distorted oxygen hexagonal layers are labeled as *A* and *B* stacking. By adapting the Thompson's notation [29], the sense of rotation of the distorted hexagon for each oxygen layer can be determined (**Figure 2(c)**). Hence, the successive oxygen layers with *AB* stacking (one ML step) create an opposing rotation, either inwardly or outwardly (**Figure 2(d)**), while the *AA*(*BB*) oxygen stacking (two ML step) would have the same rotation direction either clockwise or counter-clockwise [26, 29]. On the other hand, the coulombic repulsion between Al^{3+} cation causes each to move slightly toward the adjacent unoccupied octahedral site along the [0001] direction (perpendicular to the (0001) basal plane). This results in the formation of slightly puckered layer of Al in the basal plane, where it follows

a face-centered cubic-type *abc* stacking. Taking into account the periodic spacing of both the cation and anion layers, the structure repeats itself after six oxygen layers and six double layers of Al^{3+} cation (= 0.1299 nm) [28]. Therefore, the step height between the *A* and *B* oxygen stacking is equal to 0.217 nm as the monolayer step (**Figure 2(b)**). Moreover, no such opposing in-plane rotational geometry can be deduced from the successive Al hexagon layers in contrast to that of the distorted oxygen hexagons, suggesting that the origin of SAGB comes from the oxygen-terminated surface of sapphire substrate.

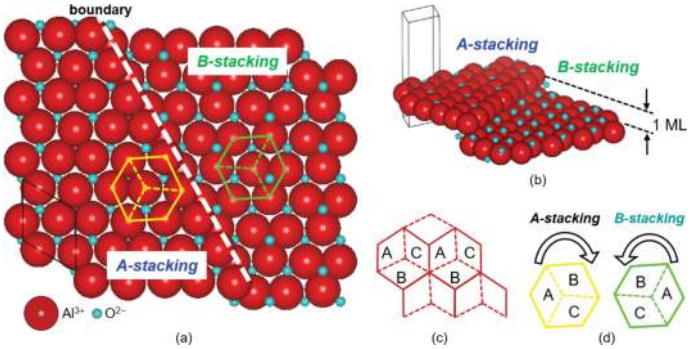

Figure 2. (a) Schematic of distorted oxygen hexagon layers in *A* and *B* stacking. (b) Side view of the *A* and *B* oxygen stacking showing the one monolayer step height. (c) Adaptation of the Thompson's notation to identify the rotation of the distorted oxygen hexagons. (d) Identification of rotation of distorted hexagons from *A* and *B* oxygen stacking layer.

To confirm this hypothesis, the AlN epilayer was grown directly on thermally cleaned sapphire substrate, which is having a monolayer step-and-terrace structure. The AlN growth temperature was 1285°C and the AlN thickness was about 0.9 μm. The atomic force microscopy (AFM) surface morphology of AlN (**Figure 3(a)**) indicates step-and-terrace structure which replicates the surface of thermally cleaned sapphire substrate. The x-ray diffraction

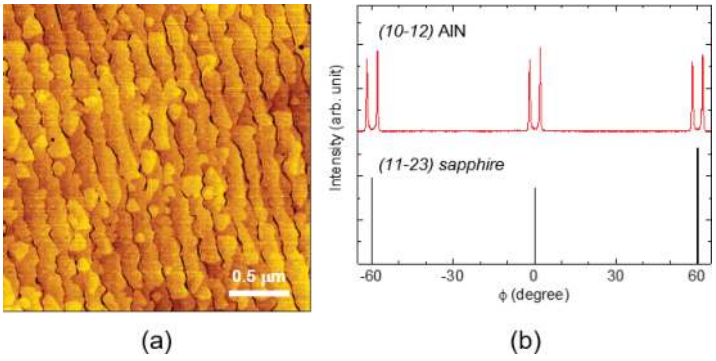

Figure 3. (a) AFM surface morphology of AlN grown directly on thermally annealed sapphire substrate (T_g = 1285°C). (b) (10-12) XRD ϕ-scan of AlN showing twin peaks which correspond to two AlN grains rotated in the in-plane. The (11-23) phi-scan of the sapphire substrate is also shown.

http://dx.doi.org/10.5772/66177

(XRD) ϕ-scan measurement of the AlN (10-12) asymmetric plane observed two peaks, which is attributed to the two periodic grains in AlN, as shown in **Figure 3(b)**. Moreover, because the XRD ϕ-scan did not show any double domain structure from the sapphire substrate, the periodic domain is only observed in the AlN epilayer. In the previous study using similar growth method, cross-sectional transmission electron microscope (TEM) analysis confirmed the existence of two grains as indicated by their periodic bright and dark contrast [26]. The plan-view high-resolution TEM observation further shows an array of edge dislocations along the grain boundary between the two AlN grains [26]. Hence, the monolayer step *ABAB* oxygen stacking is likely the origin of the small-angle grain boundary. Therefore, the surface structure of the sapphire substrate must be prevented from having such structure or modified in order to effectively eliminate the SAGB.

Several techniques have been introduced to eliminate the rotation domain. These include pre-nitrogen radical treatment of the nitrided sapphire substrate [19] and post-annealing after AlN growth [20]. However, these techniques not only entail an additional process but also obtain unsatisfactory results. Another technique is by thermal annealing in the air of sapphire substrate [26]. With the proper annealing temperature and off-cut angle, a substrate surface with *AA*(*BB*) stacking and two monolayer step height can be achieved through step bunching. On the other hand, while the TMA preflow [25] and the LT-AlN BL with pre-nitridation [21] seem promising in situ methods to eliminate the small-angle grain boundary, the influence of substrate's surface structure on its formation/elimination is not yet investigated in detail. Hence, the fragmentary understanding of the influence of surface structure is also evident after the substrate is being subjected to thermal cleaning prior to AlN growth [11, 14, 16, 18, 21, 24] or the lack of it [10, 13, 15, 22, 25]. Therefore, in this chapter, we study the influence of surface structure of sapphire substrate on the formation/elimination of SAGB to improve the quality of AlN epilayer. Then, we introduce the low-temperature (LT) AlN buffer layer technique, with emphasis on its proper timing, to eliminate the SAGB.

3. Experimental methodology

The AlN epilayers were grown on (0001) sapphire substrate by metal-organic vapor phase epitaxy. Trimethylaluminum (TMA) and NH_3 were used as source precursors for Al and N, respectively, while H_2 was used as the carrier gas. The total reactor pressure was kept at ~12 Torr. During the LT-AlN BL growth, the NH_3 and TMA flowrates were set to 1000 and 55 sccm, respectively; while, during HT-AlN growth, the NH_3 and TMA flowrates were set to 130 and 45 sccm, respectively. To study the influence of substrate's surface on the structural as well as optical quality of AlN, the temperature profiles depicted in **Figure 4** (*Profile a* and *Profile b*) were employed. For AlN growth under *Profile a*, the substrate thermal cleaning was introduced for 10 min under H_2 ambient at the same optimized growth temperature for HT-AlN (T_g =1285°C). Then the temperature was lowered to 1100°C for the growth of ~15-nm-thick LT-AlN BL. The temperature was then increased to 1285°C for the growth of ~1-μm-thick HT-AlN. For growth under *Profile b*, thermal cleaning was not introduced. Rather, the temperature was immediately brought to the desired BL T_g (800-1100°C) for the growth of

~15-nm-thick LT-AlN BL. Then the temperature was increased to T_g = 1285°C for HT-AlN growth. In the experiment, all temperature readings are from those indicated by the thermocouple placed near the substrate. Note that although both profiles incorporate LT-AlN BL, the timing, hence, the substrate's surface structure at which the LT-AlN BL is introduced is quite different, which is crucial for the formation/elimination of small-angle grain boundary. For analyses, atomic force microscopy (AFM) measurements were conducted to study the surface morphologies both of the substrate's surface and AlN epilayer, while XRD and transmission electron microscope (TEM) measurements were conducted to study the structural qualities and to assess the SAGB. CL measurements were conducted to study the optical properties of AlN.

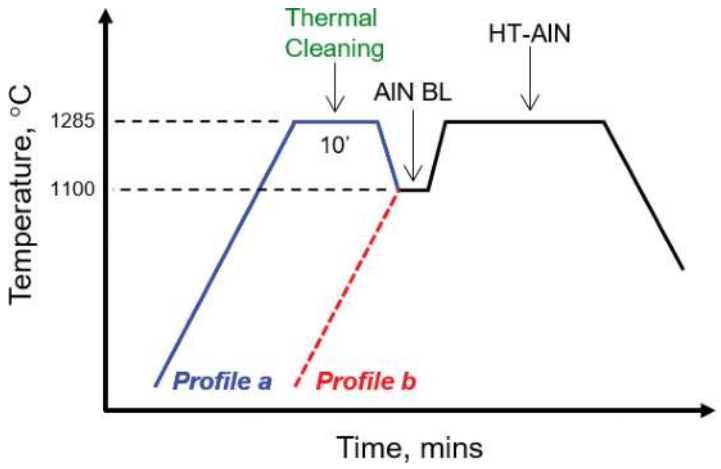

Figure 4. Temperature profiles for two-step growth of AlN on sapphire substrate. *Profile a* incorporates thermal cleaning, while *Profile b* incorporates no thermal cleaning.

4. Results and discussion

Let us then discuss the surface structure of the substrate after thermal cleaning under *Profile a* and before LT-AlN BL growth under *Profile b*. (For this case, the substrate was immediately cooled down, removed from the reactor, and analyzed.) As confirmed by AFM measurements, the thermal annealing under *Profile a* produced a parallel step-and-terrace surface structure with monolayer steps (**Figure 5(a)**). The average terrace-width and step height are ~125 and ~0.21 nm, respectively, as estimated from AFM line scan profile. Hence, the substrate's offcut angle was estimated to be ~0.11°, which is comparable to the expected off-cut angle of 0.15°. Moreover, because the ML step height corresponds to 1.299 nm $c_o/6$ = 0.22 nm, where c_o is the unit cell of sapphire having six ML steps of oxygen layers along the *c* axis [27], this confirms that the steps are correlated with the periodicity of oxygen and the interaction between oxygen atoms of successive layers is stronger than Al atoms of successive layers [26, 28].

http://dx.doi.org/10.5772/66177

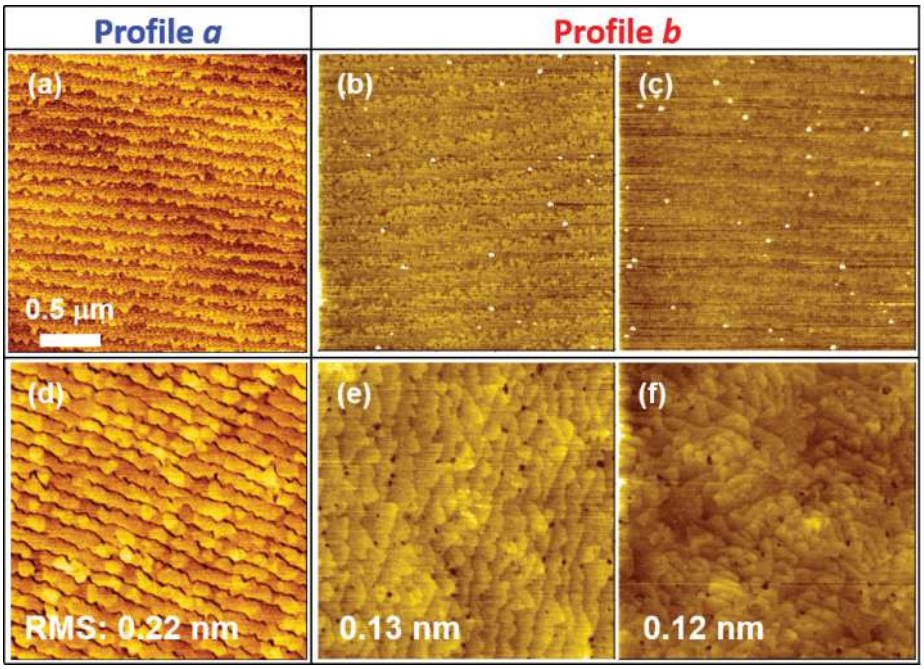

Figure 5. AFM surface morphologies of sapphire substrate after (a) thermal cleaning under *Profile a*, and before LT-AlN BL growth at (b) 1100°C and (c) 800°C under *Profile b*. The corresponding (d) HT-AlN growth for thermally cleaned substrate and under *Profile b* using (e) 1100°C and (f) 800°C LT-AlN BL T_g.

On the other hand, for sapphire substrate under *Profile b*, the formation of surface steps are undefined at BL T_g= 800°C (**Figure 5(c)**). However, two monolayer steps can be defined when the BL T_g is increased to 1100°C (**Figure 5(b)**). This indicates that with increasing BL T_g, the surface structure changes from "rough" to smooth having two ML steps. Therefore, different surface structures of sapphire substrate are formed depending on these two experimental conditions. It is therefore interesting to find out its effect on the structural quality of the subsequently grown AlN epilayer.

The corresponding surface morphologies for AlN grown under *Profile a* (**Figure 5(d)**) and *Profile b* at LT-AlN BL T_g=1100°C (**Figure 5(e)**) and 800°C (**Figure 5(f)**) are also shown in **Figure 5**. It can be seen that both profiles show an AlN with atomically smooth surfaces, as evidenced by their root-mean-square (RMS) roughness values. Moreover, a step-and-terrace surface morphology structure which replicates that of the substrate is exhibited for AlN grown under *Profile a*, while a meandering surface morphology is observed for AlN grown under *Profile b* using LT-AlN BL T_g=800°C (**Figure 5(f)**). Furthermore, these meandering steps begin to align along a certain direction as LT-AlN BL T_g is increased to 1100°C (**Figure 5(e)**). Clearly, these differences in AlN morphologies are most likely influenced by the surface structure of the substrate prior to AlN growth.

Figure 6 shows the asymmetric (10-12) ϕ-scan of AlN epilayers grown under *Profile a* (**Figure 6(a)**) and *Profile b* using LT-AlN BL T_g=1100°C (**Figure 6(b)**). The (11-23) ϕ-scan of the substrate is also shown. It is well known that the in-plane epitaxial relationship between AlN and sapphire is AlN<10-10>||α-Al_2O_3<11-20> [8]. Moreover, a closer look at AlN (10-12) diffraction shows two peaks under *Profile a* (**Figure 6(a)**) with separation $\Delta\theta \sim 3.72°$, while only a single diffraction peak is observed under *Profile b*. This indicates the presence of a special grain boundary under *Profile a*, where the two AlN grains have a particular in-plane misorientation relationship, while it is successfully suppressed under *Profile b*. Furthermore, because sapphire (11-23) diffraction does not exhibit two peaks, the special grain boundary is confirmed to exist only in AlN epilayer.

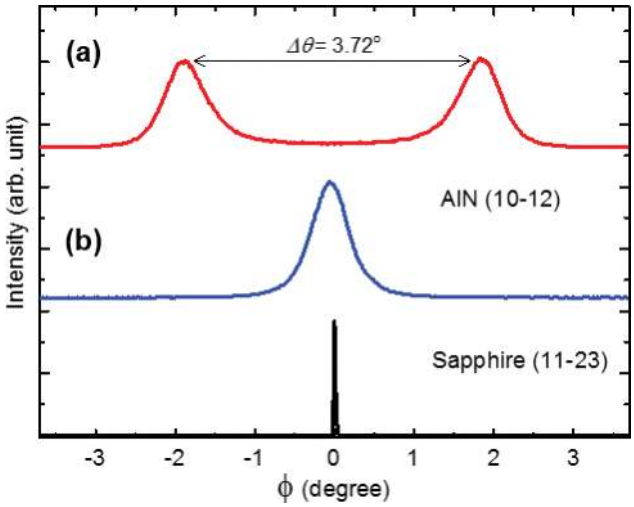

Figure 6. XRD ϕ-scans of AlN grown sapphire substrate under (a) *Profile a* and (b) *Profile b* using LT-AlN BL T_g= 1100°C.

To further confirm the existence of the special grain boundary in AlN under *Profile a*, a plan-view bright-field TEM micrograph and the corresponding selected area electron diffraction pattern (SAEDP) were taken under [0001] zone axis, as shown respectively in **Figures 7(a)** and **(b)**. A periodic bright and dark contrast of two AlN grains is observed. The AlN grain width is found identical to the step width of thermally cleaned sapphire substrate, implying that the origin of the grain boundary is related to the substrate's surface structure. As the AlN is grown onto sapphire substrate with either *A* or *B* oxygen stacking, the characteristic of that surface is also carried into AlN [26]. And as supported by XRD results and because only a slight misorientation relative to one another exists between these two AlN grains, this grain boundary is confirmed to be a small-angle grain boundary [25, 26]. Furthermore, due to the arrays of edge dislocations that exist at the boundary, this type of special boundary is called pure low-angle tilt SAGB. The spacing D between adjacent edge dislocation array can also be estimated using the formula $D = \mathbf{b}/\sin\theta \approx \mathbf{b}/\sin\Delta\theta$, where $\mathbf{b}$ is the in-plane burger's vector

http://dx.doi.org/10.5772/66177

(= 0.3112 nm) and $\Delta\theta$ is the misorientation angle ($\Delta\theta \sim 3.72°$) obtained from XRD measurement. Hence, the spacing between edge dislocations is estimated to be ~4.75 nm. The SAEDP also supports the observation of SAGB, as seen from the double diffraction spots (denoted by arrow marks in **Figure 7(b)**). On the other hand, no special grain boundary is observed for AlN grown under *Profile b* (not shown). This suggests that the buffer layer technique is effective for suppressing the SAGB.

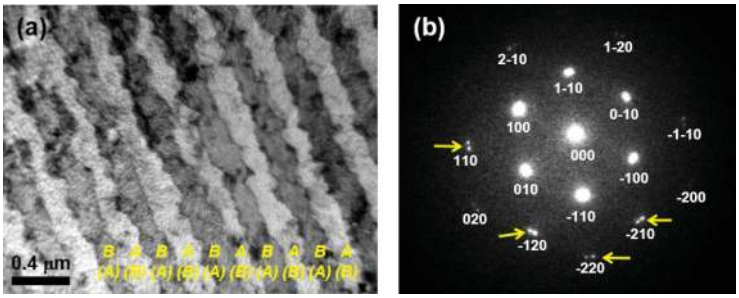

Figure 7. Plan-view TEM bright-field image of AlN grown under (a) *Profile a*. (b) Corresponding selected-area electron diffraction pattern of AlN in (a).

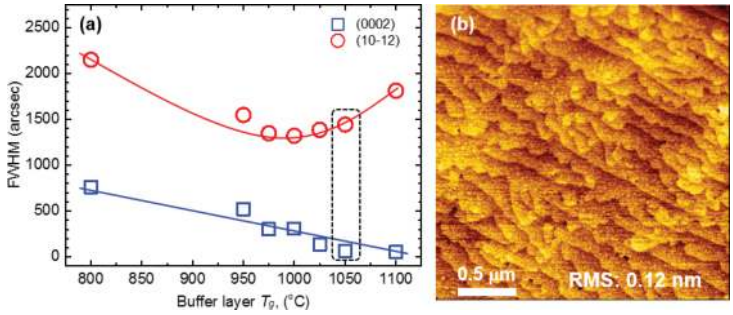

Figure 8. (a) LT-AlN BL T_g as a function of symmetric (0002) and asymmetric (10-12) ω-scans. (b) AFM surface morphology of AlN grown at optimum LT-AlN BL T_g (1050°C).

Then the LT-AlN BL T_g was optimized to improve the mosaicity of the epitaxial film using the current growth condition. The result of the XRD symmetric (0002) and asymmetric (10-12) ω-scans are shown in **Figure 8**. While the XRD linewidth of the tilt component corresponding to the symmetric (0002) becomes narrow with increasing temperature, the twist component corresponding to the asymmetric (10-12) initially becomes narrow and then broadens with increasing temperature. Hence, the narrowest linewidth for each component does not coincide with each other, and the reason is still unknown at this time. But by balancing these components, it can be deduced that the optimum LT BL temperature is T_g ~1050°C, where the XRD linewidths are ~66 and ~1443 arcsec, respectively, for (0002) and

(10-12) ω-scans. The symmetric component is comparable to that grown under *Profile a* (FWHM is ~64 arcsec), suggesting that both have highly-oriented films along the *c*-axis growth direction. On the other hand, the asymmetric (10-12) linewidth is wider than that grown under *profile a* (FWHM is 1145 arcsec). **Figure 8(b)** shows the AFM surface morphology of AlN grown under the optimum LT-AlN BL T_g of 1050°C. Although nanopits have been reduced compared with other BL T_g (**Figures 5(e)**, **(f)**), it is believed that the quality of the film can be further improved especially the twist mosaicity upon optimizing the buffer layer thickness or other growth parameters.

To demonstrate the effect of eliminating the SAGB on the optical properties of AlN epilayer, we obtained the CL spectra for both profiles, as shown in **Figure 9**. The CL measurements were acquired at 93 K under 10 kV and 0.1 μA emission condition (spot size is ~1 μm). CL peaks are assigned to free and bound excitonic emissions, including the LO phonon replicas, as shown in the inset figure [14]. Moreover, the emission intensity of AlN under *Profile b* using the optimum LT-AlN BL T_g of 1050°C is approximately more than two times higher than that under *Profile a*. This result is attributed to the higher probability of radiative recombination of electron and hole pairs due to the elimination small-angle grain boundary. The differences in the CL peak position also suggest their different residual strain, where the tensile-strained AlN under *Profile b* has smaller bandgap energy (~6.011 eV) than that of an almost relaxed AlN (~6.031 eV) under *Profile a*. The slow relaxation experienced by AlN under *Profile b* is most likely due to the reduced generation of dislocations upon the suppression of SAGB. As SAGB is a type of an edge dislocation, eliminating it is expected to enhance the optical properties of AlN.

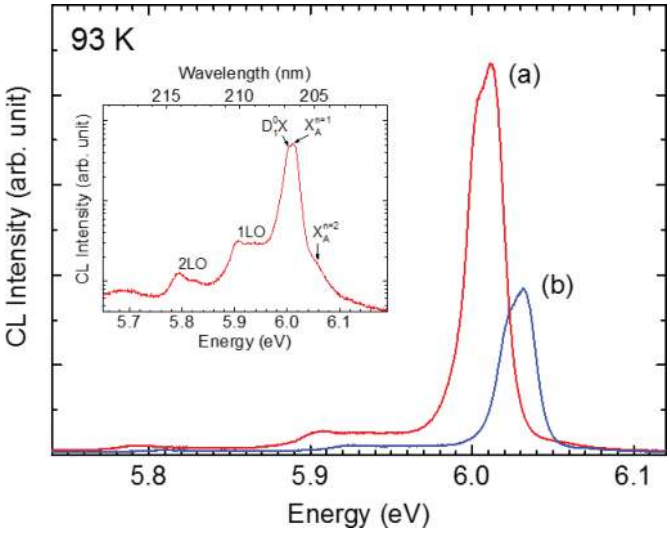

Figure 9. CL spectra of AlN grown under (a) *Profile a* and (b) *Profile b* using optimum LT-AlN BL T_g = 1050°C.

http://dx.doi.org/10.5772/66177

Hence, the origin of SAGB can be ascribed to the surface structure of sapphire substrate. It was shown that as long as the surface has ML steps, even the introduction of LT-AlN BL would be ineffective in eliminating the SAGB. Hence, there is a maximum allowable BL T_g at which the substrate's surface does not transform into monolayer steps yet. In this study, we consider that the maximum BL T_g would be around 1100°C. The result also implies that there is a proper timing to introduce the LT-AlN BL [21]. This tendency is also observed in direct HT-AlN growth using different growth methods [16, 21, 25], suggesting the wide observation of this phenomenon. It is noteworthy that even during temperature ramp-up, because the optimal T_g for HT-AlN growth is in the vicinity around T_g = 1200°C, it is likely that the surface could also change to periodic (ML) steps, as pointed out [25]. This is also supported in the present study based on the evolution of surface structure in both profiles. Therefore, the LT-AlN BL would be necessary in order to prevent the surface from transforming into structures with monolayer steps. Conversely, with the application of LT-AlN BL, the two ML steps observed using LT-AlN BL T_g = 1100°C is kept, hence, preserving their heteroepitaxial relationship (as expected, 2 ML steps do not form SAGB). For BL T_g = 800°C, it is believed that the "weak" heteroepitaxial relationship due to the undefined (rough) surface plays a role in circumventing the SAGB.

On the other hand, the SAGB can also be prevented even when using thermally cleaned substrate. In fact, a lot of AlN growth optimizations have been performed under such condition and yet, there was no observation of SAGB or hardly any mention if at all. The reason could be due to the weakening of the epitaxial relationship between the sapphire and AlN after introducing some extrinsic factors such as nitridation before LT-AlN BL or AlN seeding layer [11, 14, 26]. This could be the reason why the growth interruption by V/III ratio resulted in not only dislocation bending or coalescence but also the elimination of domain structure [18, 24]. Moreover, the insertion of an intermediate layer after LT-AlN BL could have also eliminated the rotation domain [30]. In addition, the no observation of rotation domain on thermally cleaned substrate would also depend on thermal cleaning temperature or temperature ramp-up. In their study, substrate surface after thermal cleaning at 1145°C prior to LT-AlN BL growth could have 2 ML step structure, thus preventing the SAGB [23]. Also, the initial supply of TMA (TMA preflow) during the pulse growth could have replaced the oxygen-terminated surface into Al-terminated one [25]. As mentioned earlier, the sapphire's surface with Al termination is expected to have no rotation domain.

Finally, **Table 1** shows the comparison between several techniques for eliminating the SAGB performed on as-received and nitrided sapphire substrates. Note that techniques included in the table are only those that directly discussed the rotation domain. Although a high-quality AlN could be obtained from nitrided sapphire substrate, residual SAGB still exists, albeit coalesced with other domain upon nitrogen radical or annealing treatment [19, 20]. Moreover, the step bunching of sapphire substrate into $n \times 2$ ML, where n is an integer, would require a critical off-cut angle during *ex situ* surface treatment [26]. On the other hand, the LT-AlN BL technique would eliminate these additional processes owing to its in situ treatment. It is noteworthy that although rotation domain phenomenon was not observed in previous studies using LT-AlN BL, we believe that whether intentionally or unintentionally, the elimination of rotation domain is one of its underlying purposes. For example, Xi et al. adopted this approach,

and a high-quality and atomically smooth AlN epilayer was obtained [22]. The same is true in the work of Zhang et al.; however, they introduced the PALE approach to enhance the migration of Al adatoms during the HT-AlN growth [15]. But Hu et al. modified this method by performing nitridation pretreatment under H_2/NH_3 ambient prior to LT-AlN BL growth. However, they ascribed the elimination of rotation domain to the different strain relaxation mechanisms induced by lattice mismatch [21]. In addition, nitridation pretreatment may induce rough AlN surface. Therefore, LT-AlN BL is a promising technique for eliminating the rotation domain. It is noteworthy that LT BL has been used as a standard technique for the growth of GaN, resulting in crack-free and high-quality epilayer [31, 32]. However, to the best of our knowledge, this is the maiden report that clarifies the role of LT-AlN BL for obtaining high-quality AlN without SAGB.

Sapphire substrate	Pre/post-treatment technique	Suppression of SAGB	Smooth surface	In situ treatment
As-received	LT AlN BL without thermal cleaning (present technique)	+	+	+
As-received	TMA preflow [25]	+	+	+
	NH_3 preflow [25]	-	+	+
As-received	LT AlN BL with thermal cleaning [21]	-	+/-	+
	Nitridation and LT AlN BL [21]	+	+/-	+
As-received	Thermal cleaning [16, 26]	-	+	+
As-received	Annealing in air [26]	+	+	-
Nitrided	Annealing [20]	-	-	+
Nitrided	Nitrogen radical treatment [19]	-	-	+

Table 1. Comparison among several techniques reported for eliminating SAGB in AlN, where "+" sign shows the satisfied property, and the "-" sign shows the unsatisfied property.

5. Summary

In summary, the surface structure of sapphire substrate is found to influence the formation of small-angle grain boundary in subsequently grown AlN epilayer. The small-angle grain boundary is formed when the surface of the sapphire (0001) substrate is terminated by *ABAB* oxygen stacking with monolayer steps, which is formed during high-temperature thermal cleaning. To circumvent the small-angle grain boundary, the LT-AlN BL is introduced in order to circumvent the substrate structure from having monolayer steps. Rather, the substrate surface produced either rough structure at low BL T_g or defined two-ML-step structure as LT-AlN BL T_g is increased. CL measurement showed an increased emission from the AlN without SAGB. Thus, the LT-AlN BL technique would be effective in eliminating the SAGB, thereby obtaining high-quality AlN epilayer with improved optical and electrical properties.

Acknowledgements

The authors acknowledge Dr. M. Sumiya, Dr. K. Watanabe, and Dr. N. Ishida for their helpful discussions and assistance throughout this work.

Author details

Ryan G. Banal*, Masataka Imura* and Yasuo Koide*

*Address all correspondence to: BANAL.Ryan@nims.go.jp, IMURA.Masataka@nims.go.jp and KOIDE.Yasuo@nims.go.jp

Wide Bandgap Materials Group, National Institute for Materials Science (NIMS), Namiki, Tsukuba, Ibaraki, Japan

References

[1] Grandusky J.R., Smart J.A., Mendrick M.C., Schowalter L.J., Chen K.X., Schubert E.F. Pseudomorphic growth of thick n-type AlxGa1-xN layers on low-defect-density bulk AlN substrates for UV LED applications. Journal of Crystal Growth. 2009;311(10):2864–2866. DOI: 10.1016/j.jcrysgro.2009.01.101

[2] Rice A., Collazo R., Tweedie J., Dalmau R., Mita S., Xie J., et al. Surface preparation and homoepitaxial deposition of AlN on (0001)-oriented AlN substrates by metalorganic chemical vapor deposition. Journal of Applied Physics. 2010;108:043510:1–8. DOI: 10.1063/1.3467522

[3] Sugahara T., Sato H., Hao M., Naoi Y., Kurai S., Tottori S., et al. Direct evidence that dislocations are non-radiative recombination centers in GaN. Japanese Journal of Applied Physics. 1998;37(Part 2, Number 4A):L398–L400. DOI: 10.1143/JJAP.37.L398

[4] Khan A., Balakrishnan K., Katona T. Ultraviolet light-emitting diodes based on group three nitrides. Nature Photonics. 2008;2:77–84. DOI: 10.1038/nphoton.2007.293

[5] Shatalov M., Sun W., Jain R., Lunev A., Hu X., Dobrinsky A., et al. High power AlGaN ultraviolet light emitters. Semiconductor Science and Technology. 2014;29(8):084007. DOI: 10.1088/0268-1242/29/8/084007

[6] Hirayama H., Maeda N., Fujikawa S., Toyoda S., Kamata N. Recent progress and future prospects of AlGaN-based high-efficiency deep-ultraviolet light-emitting diodes. Japanese Journal of Applied Physics. 2014;53(10):100209:1–10. DOI: 10.7567/JJAP.53.100209

[7] Li X.-H., Kao T.-T., Satter Md.M., Wei Y.O., Wang S., Xie H., et al. Demonstration of transverse-magnetic deep-ultraviolet stimulated emission from AlGaN multiple-quantum-well lasers grown on a sapphire substrate. Applied Physics Letters. 2015;106:04115:1–4. DOI: 10.1063/1.4906590

[8] Vispute R.D., Wu H., Narayan J. High quality epitaxial aluminum nitride layers on sapphire by pulsed laser deposition. Applied Physics Letters. 1995;67:1549–1551. DOI: 10.1063/1.114489

[9] Hiroki M., Kobayashi N. Flat Surfaces and interfaces in AlN/GaN heterostructures and superlattices grown by flow-rate modulation epitaxy. Japanese Journal of Applied Physics. 2003;42(Part 1, Number 4B):2305–2308. DOI: 10.1143/JJAP.42.2305

[10] Adivarahan V., Sun W.H., Chitnis A., Shatalov M., Wu S., Maruska H.P., et al. 250 nm AlGaN light-emitting diodes. Applied Physics Letters. 2004;85:2175–2177. DOI: 10.1063/1.1796525

[11] Takeuchi M., Shimizu H., Kajitani R., Kawasaki K., Kumagai Y., Koukitu A., et al. Improvement of crystalline quality of N-polar AlN layers on c-plane sapphire by low-pressure flow-modulated MOCVD. Journal of Crystal Growth. 2007;298:336–340. DOI: 10.1016/j.jcrysgro.2006.10.140

[12] Hirayama H., Yatabe T., Noguchi N., Ohashi T., Kamata N. 231 – 261 nm AlGaN deep-ultraviolet light-emitting diodes fabricated on AlN multilayer buffers grown by ammonia pulse-flow method on sapphire. Applied Physics Letters. 2007;91:071901:1–3. DOI: 10.1063/1.2770662

[13] Zhang J.P., Khan M.A., Sun W.H., Wang H.M., Chen C.Q., Fareed Q., et al. Pulsed atomic-layer epitaxy of ultrahigh-quality AlxGa1-xN structures for deep ultraviolet emissions below 230 nm. Applied Physics Letters. 2002;81:4392–4394. DOI: 10.1063/1.1528726

[14] Takeuchi M., Ooishi S., Ohtsuka T., Maegawa T., Koyama T., Chichibu S.F., et al. Improvement of Al-Polar AlN layer quality by three-stage flow-modulation metalorganic chemical vapor deposition. Applied Physics Express. 2008;1(Number 2): 021102:1–021102:3. DOI: 10.1143/APEX.1.021102

[15] Zhang J.P., Wang H.M., Sun W.H., Adivarahan V., Wu S., Chitnis A., et al. High-quality AlGaN layers over pulsed atomic-layer epitaxially grown AlN templates for deep ultraviolet light-emitting diodes. Journal of Electronic Materials. 2003;32(5):364–370. DOI: 10.1007/s11664-003-0159-2

[16] Banal R.G., Funato M., Kawakami Y. Initial nucleation of AlN grown directly on sapphire substrates by metal-organic vapor phase epitaxy. Applied Physics Letters. 2008;92:241905:1–241905:3. DOI: 10.1063/1.2937445

[17] Ohba Y., Yoshida H., Sato R. Growth of High-Quality AlN, GaN and AlGaN with atomically smooth surfaces on sapphire substrates. Japanese Journal of Applied Physics. 1997;36(Part 2, Number 12A):L1565–L1567. DOI: 10.1143/JJAP.36.L1565

[18] Imura M., Nakano K., Fujimoto N., Okada N., Balakrishnan K., Iwaya M., et al. High-temperature metal-organic vapor phase epitaxial growth of AlN on sapphire by multi transition growth mode method varying V/III ratio. Japanese Journal of Applied Physics. 2006;45(Part 1, Number 11):8639–8643. DOI: 10.1143/JJAP.45.8639

[19] Ueno K., Ohta J., Fujioka H., Fukuyama H. Characteristics of AlN films grown on thermally-nitrided sapphire substrates. Applied Physics Express. 2010;4(Number 1): 015501:1–015501:3. DOI: 10.1143/APEX.4.015501

[20] Adachi M., Sugiyama M., Tanaka A., Fukuyama H. Elimination of rotational domain in AlN layers grown from Ga–Al flux and effects of growth temperature on the layers. Materials Transactions. 2012;53(Number 7):1295–1300. DOI: 10.2320/matertrans.MBW201112

[21] Wang H., Xiong H., Wu Z.-H., Yu C.-H., Tian Y., Dai J.-N., et al. Occurrence and elimination of in-plane misoriented crystals in AlN epilayers on sapphire via pretreatment control. Chinese Physics B. 2013;23(Number 2):028101:1–028101:5. DOI: 10.1088/1674-1056/23/2/028101

[22] Xi Y.A., Chen K.X., Mont F., Kim J.K., Wetzel C., Schubert E.F., et al. Very high quality AlN grown on (0001) sapphire by metal-organic vapor phase epitaxy. Applied Physics Letters. 2006;89:103106:1–103106:3. DOI: 10.1063/1.2345256

[23] Lai M.-J., Chang L.-B., Yuan T.-T., Lin R.-M. Improvement of crystal quality of AlN grown on sapphire substrate by MOCVD. Crystal Research and Technology. 2010;45(7): 703–706. DOI: 10.1002/crat.201000063

[24] Peng M.-Z., Guo L.-W., Zhang J., Yu N.-S., Zhu X.-L., Yan J.-F., et al. Three-step growth optimization of AlN epilayers by MOCVD. Chinese Physics Letters. 2008;25(Number 6):2265–2268. DOI: 10.1088/0256-307X/25/6/094

[25] Kawaguchi K., Kuramata A. Defect structures of AlN on sapphire (0001) grown by metalorganic vapor-phase epitaxy with different preflow sources. Japanese Journal of Applied Physics. 2005;44(Part 2, Numbers 46–49):L1400–L1402. DOI: 10.1143/JJAP.44.L1400

[26] Hayashi Y., Banal R.G., Funato M., Kawakami Y. Heteroepitaxy between wurtzite and corundum materials. Journal of Applied Physics. 2013;113:183523:1–183523:8. DOI: 10.1063/1.4804328

[27] Chiang Y.-M., Birnie III D., Kingery W.D. Physical Ceramics: Principles for Ceramic Science and Engineering. Canada: Wiley & Sons, Inc.; 1997. 540 p.

[28] Van L.P., Kurnosikov O., Cousty J. Evolution of steps on vicinal (0001) surfaces of α-alumina. Surface Science. 1998;411(3):263–271. DOI: 10.1016/S0039-6028(98)00329-X

[29] Berghezan A., Fourdeaux A., Amelinckx S. The structure and properties of grain boundaries. Acta Metallurgica. 1961;9(5):464–490. DOI: 10.1016/0001-6160(61)90142-0

[30] Cai B., Nakarmi M.L. TEM analysis of microstructures of AlN/sapphire grown by MOCVD. In: Gwo S., Ager J.W., Ren F., Ambacher O., Schowalter L., editors. MRS Proceedings; November 30–December 4, 2009; Boston, Massachusetts. Materials Research Society; 2010. pp. 1202-I05:01–1202-I05:05. DOI: 10.1557/PROC-1202-I05-01

[31] Amano H., Sawaki N., Akasaki I., Toyoda Y. Metalorganic vapor phase epitaxial growth of a high quality GaN film using an AlN buffer layer. Applied Physics Letters. 1986;48:353–355. DOI: 10.1063/1.96549

[32] Nakamura S. GaN growth using GaN buffer layer. Japanese Journal of Applied Physics. 1991;30(Part 2, Number 10A):L1705–L1707. DOI: 10.1143/JJAP.30.L1705